Article

Transient and Fast Generation of Bose-Einstein-Condensate Macroscopic Quantum Superposition States via Impurity Catalysing

Zhen Li [1] and Wangjun Lu [2,*]

[1] Department of Physics, Shaoyang University, Shaoyang 422099, China
[2] Department of Maths and Physics, Hunan Institute of Engineering, Xiangtan 411104, China
* Correspondence: wjlu@hnie.edu.cn

Abstract: Macroscopic quantum superposition is an important embodiment of the core of the quantum theory. The engineering of macroscopic quantum superposition states is the key to quantum communication and quantum computation. Thus, we present a theoretical proposal to engineer macroscopic quantum superposition (MQS) states of a Bose-Einstein condensate (BEC) via impurity atoms. We firstly propose a deterministic generation scheme of transient multi-component MQS states of the BEC via impurity catalysing. It is found that the structure of the generated transient multi-component MQS states can be manipulated by the impurity number parity. Then, we illustrate the influence of impurity number parity on MQS states through three aspects: generation of approximately orthogonal continuous-variable cat states, manipulation of non-classicality in phase space, and switching of non-classical degree of BEC states. The influence of the BEC decoherence on the generation of MQS states is discussed by the fidelity between actually generated states and target states. Finally, the results show that the high-fidelity multi-component MQS states of the BEC can be fast generated by increasing the coherent interaction strength between impurities and the BEC in an open system.

Keywords: macroscopic quantum superposition; quantum communication; Bose-Einstein condensate; impurity; catalysing

1. Introduction

It is an important feature of quantum physics that objects can exist in the form of coherent superposition of different quantum states [1]. Such quantum superposition is also an essential signal that distinguishes the quantum from the classical world [2]. Quantum physics has long been regarded as a theory describing the motion of objects at microscopic scales. Thus, the superpositions of macroscopically distinct quantum states have been a good prospect. This kind of quantum superposition states was previously discussed by Schrödinger in his paradox and is often subsequently called Schrödinger's cat states [3]. Apart from fundamental tests of quantum mechanics [4–6], macroscopic quantum superposition (MQS) states have been shown to enable quantum computation [7–11], quantum metrology [12–14], quantum repeaters [15], and quantum teleportation [16]. Thus, much attention has been paid to preparation, engineering, control, and detection of such MQS states for several decades [17–22]. A Bose-Einstein condensate (BEC) [23–25] has emerged as a pristine platform for studying MQS states due to the macroscopic nature of its wave function and the tunability of the interatomic interaction at will. Several approaches [26–38] have been suggested to produce such MQS states .

Recently, the physics of impurity-doped Bose-Einstein condensate (BEC) systems have made great progress in experiments [39–43]. A BEC with immersed impurities provides a totally new platform for studying quantum phenomena of the micro-macro hybrid quantum systems, for instance, the impurity-induced Dicke quantum phase transition [44],

macroscopic quantum resource[45–47], the BEC decoherence probe [48] and phase fluctuations [49], and quantum decoherence speed limit [50].

The purpose of the present paper is to propose a theoretical scheme to engineer MQS states of the BEC through the impurity atoms. We consider an impurity-doped BEC system with N two-level impurity atoms, such as Rydberg atoms with the ground state and excited Rydberg state being two energy levels, respectively [51,52]. Based on the Rydberg impurity-doped BEC system, we will show how to deterministically create the transient BEC multi-component MQS states by the dynamically decoupling of the impurity atoms from the BEC. We indicate that MQS states of the BEC can be engineered via the impurity atoms. We find that the impurity number parity has a significant impact on BEC state parameters, phase space distribution as well as non-classical degree. In addition, the increasing impurities-BEC interaction strength can reduce preparation time. In particular, this will weaken the destructive effects of the environment on the quantum system for an open system. Numerical results display that the fast generation [53] of high-fidelity MQS states can be obtained.

The remainder of this paper is organized as follows. In Sec. II, we introduce the impurity-doped BEC model consisting of BEC and N identical Rydberg impurity atoms and present the analytical solution of the impurity-doped BEC model. Section III shows how to deterministically generate transient multi-component MQS states of the BEC. The manipulation of impurity number parity on MQS states is presented in Sec. IV. Section V explains how the interaction between impurities and BEC induces the fast generation of high-fidelity MQS states in an open system. Finally, Sec. VI is devoted to some concluding remarks.

2. The Impurities-Doped BEC Model

We consider an impurity-doped BEC system which consists of the BEC and N two-level impurity atoms. We assume that the N fixed impurities are immersed in the BEC, and the number of the impurities is much smaller than the number of the condensed atoms in the BEC. Under these conditions, the interaction between impurity atoms can be neglected. The Hamiltonian of the BEC in a trapping potential [23] is

$$H_B = \int d\mathbf{x}\Psi^\dagger(\mathbf{x})\left[-\frac{1}{2m}\nabla^2 + V(\mathbf{x}) + \frac{U}{2}\Psi^\dagger(\mathbf{x})\Psi(\mathbf{x})\right]\Psi(\mathbf{x}), \tag{1}$$

where $\Psi(\mathbf{x})$ is the BEC field operator, $V(\mathbf{x})$ is the external trapping potential, U is the self-interaction, and m is the mass of an atom. The condensate is assumed to be trapped in a deep potential such that the BEC can be well described within the single-mode approximation $\Psi(\mathbf{x}) \approx a\phi(\mathbf{x})$. Here a and $\phi(\mathbf{x})$ are the annihilator operator and the mode function of the condensate, respectively. Then, the Hamiltonian of the confined BEC can be written as a Kerr-type Hamiltonian

$$H_B = \omega_b a^\dagger a + \lambda a^\dagger a^\dagger aa, \tag{2}$$

where the mode frequency ω_b and the coupling strength λ are defined as

$$\omega_b = \int d\mathbf{x}\left[-\frac{1}{2m}|\nabla\phi(\mathbf{x})|^2 + V(\mathbf{x})|\phi(\mathbf{x})|^2\right], \tag{3}$$

$$\lambda = \frac{U}{2}\int d\mathbf{x}|\phi(\mathbf{x})|^4. \tag{4}$$

The impurities interact with the BEC via coherent collisions. Thus, the impurities Hamiltonian and impurity-BEC interaction Hamiltonian can be described as

$$H_{iB} = \omega_0 \sum_{i=1}^{N}\sigma_z^i + \frac{1}{2}\kappa\sum_{i=1}^{N}\sigma_z^i a^\dagger a, \tag{5}$$

where σ_z^i is a Pauli operator of i-th impurity atom, ω_0 is the transition frequency of impurity atoms between ground and excited state, and κ is the interaction strength between the impurities and BEC. We assume the free Hamiltonian $H_0 = (\omega_b - \lambda)a^\dagger a + \omega_0 \sum_{i=1}^N \sigma_z^i$. Making use of Eqs. (2) and (5), we can obtain the Hamiltonian of the total system in the interaction picture as

$$H_I = i\dot{u}u^\dagger + u(H_B + H_{iB})u^\dagger = \lambda\left(a^\dagger a\right)^2 + \kappa \hat{J}_z a^\dagger a, \tag{6}$$

where $u = \exp(iH_0 t)$ and we have introduced a collective operator of the N two-level impurities

$$J_x = \frac{1}{2}\sum_{i=1}^N \sigma_x^i, \qquad J_y = \frac{1}{2}\sum_{i=1}^N \sigma_y^i, \qquad J_z = \frac{1}{2}\sum_{i=1}^N \sigma_z^i, \tag{7}$$

which obey the following commutation relations of the $su(2)$ algebra

$$[J_x, J_y] = iJ_z, \qquad [J_y, J_z] = iJ_x, \qquad [J_z, J_x] = iJ_y, \tag{8}$$

where $J_\pm = J_x \pm iJ_y$ is the ladder operator of the angular momentum.

The Hamiltonian (6) has the following eigenvalues and eigenstates

$$E_{nm} = \lambda n^2 + \kappa nm, \qquad |\Psi\rangle_{nm} = |n\rangle \otimes |j, m\rangle, \tag{9}$$

where $|n\rangle$ is a Fock state of the BEC with $n = 0, 1, 2, \cdots, \infty$, and $|j, m\rangle$ is a common eigenstate of the operators J^2 and J_z with $j = N/2$, and $m = -j, -j+1, -j+2, \ldots j$.

3. Deterministic Creation of MQS States

3.1. Creating Multi-Component MQS States

We consider the impurity atoms and the BEC are initially in a Greenberger-Horne-Zeilinger (GHZ) state and a coherent state $|\alpha\rangle$, respectively. The GHZ state of N impurity atoms can be represented in terms of the basis of the angular momentum space as

$$\begin{aligned} |\mathbf{GHZ}\rangle &= \frac{1}{\sqrt{2}}[|00\ldots0\rangle + |11\ldots1\rangle] \\ &= \frac{1}{\sqrt{2}}[|N/2, -N/2\rangle + |N/2, N/2\rangle], \end{aligned} \tag{10}$$

where $|N/2, N/2\rangle$ and $|N/2, -N/2\rangle$ are the highest-weight and lowest-weight states in the angular momentum representation of the $su(2)$ algebra with $j = N/2$, respectively.

Then the initial state of the impurity-doped BEC system is given by

$$|\Psi(0)\rangle = \frac{1}{\sqrt{2}}[|j, -j\rangle + |j, j\rangle] \otimes |\alpha\rangle, \tag{11}$$

where $j = N/2$ and $|\alpha\rangle = D(\alpha)|0\rangle$ with the displacement operator being given by $D(\alpha) = \exp(\alpha a^\dagger - \alpha^* a)$.

Making use of Equation (6) and (9), due to the commutative relationship $[(a^\dagger a)^2, \hat{J}_z a^\dagger a] = 0$, the time evolution operator $U(t)$ can be written in the following decoupling form:

$$U(t) = \exp[-i\tau \hat{n}^2 \lambda/\kappa] \exp[-i\tau \hat{J}_z \hat{n}], \tag{12}$$

where the scaled time $\tau = \kappa t$ and then we can obtain the wave function of the impurity-doped BEC system at a scaled time τ

$$|\Psi(\tau)\rangle = \frac{1}{\sqrt{2}}\left[|\Psi(\tau)_{-j,\alpha}\rangle \otimes |j, -j\rangle + |\Psi(\tau)_{+j,\alpha}\rangle \otimes |j, j\rangle\right], \tag{13}$$

where we have introduced a impurity-dependent BEC state $|\Psi(\tau)_{\pm j,\alpha}\rangle$, which can be expressed as a form of a generalized coherent state [54–58]

$$|\Psi(\tau)_{\pm j,\alpha}\rangle = e^{-\frac{1}{2}|\alpha|^2} \sum_{n=0}^{\infty} e^{-i\tau(\lambda/\kappa)n^2} \frac{\left(\alpha e^{\mp i\tau j}\right)^n}{\sqrt{n!}} |n\rangle. \tag{14}$$

It is not difficult to find that the BEC matter field is entangled with impurities during the dynamics evolution. It's worth noting that the entanglement between BEC and impurities are periodic, and the BEC matter field will completely decoupled from the impurity atoms at $\tau = 2k\pi/N$ $(k \in Z)$.

At time $\tau = 2\pi$ and $j = N/2$, we have $\exp(\mp i\tau j) = (-1)^N$, and the entanglement between BEC and impurity atoms disappears. The state of the system becomes

$$|\Psi(\tau = 2\pi)\rangle = \frac{1}{\sqrt{2}} [|j, -j\rangle + |j, j\rangle] \otimes \left|\Psi(\tau = 2\pi)_{N,\alpha}\right\rangle, \tag{15}$$

where the impurities returns to its originally GHZ state and the state of the BEC reads

$$|\Psi(\tau = 2\pi)_{N,\alpha}\rangle = e^{-\frac{1}{2}|\alpha|^2} \sum_{n=0}^{\infty} e^{-i2\pi(\lambda/\kappa)n^2} \frac{\left[\alpha(-1)^N\right]^n}{\sqrt{n!}} |n\rangle. \tag{16}$$

$|\Psi(\tau = 2\pi)_{N,\alpha}\rangle$ is the so-called Yurke-Stoler-like state [59,60], which can be recognized as a variety of quantum superposition of Glauber coherent states for different values of λ/κ. We define $\Pi = (-1)^N$ as the impurity number parity and $\lambda/\kappa = 1/2P$ $(P = 2, 3, 4, \cdots, \infty)$. Then, the phase function in Equation (16) can be written as a sum of P terms [61]

$$e^{-i\pi n^2/P} = \frac{1}{\sqrt{P}} \sum_{k=1}^{P} \exp(i\xi_k)\left[-\exp\left(\frac{2ik\pi}{P}\right)\right]^n, \tag{17}$$

where phase factor ξ_k is related to parameter P. For example: $\xi_1 = -\pi/4$ and $\xi_2 = \pi/4$ when $P = 2$, $\xi_1 = \xi_2 = -\pi/6$ and $\xi_3 = \pi/2$ when $P = 3$. Obtaining the above results requires solving a system of equations consisting of P equations. Thus, we can get the specific value of ξ_k when the parameter P is determined by using Equation (17). There are many mathematical processes involved. According with Equation (17), $|\Psi(\tau = 2\pi)_{N,\alpha}\rangle$ is superimposed by the coherent states of P components

$$|\Psi(\tau = 2\pi)_{N,\alpha}\rangle_{1/2P} = \frac{1}{\sqrt{P}} \sum_{k=1}^{P} \exp(i\xi_k)|-\Pi\alpha \exp(2ik\pi/P)\rangle$$

$$= \frac{1}{\sqrt{P}} \sum_{k=1}^{P} \exp(i\xi_k)|\Pi\alpha_k\rangle, \tag{18}$$

where k is positive integer and $\alpha_k = -\alpha \exp(2ik\pi/P)$. $|-\Pi\alpha \exp(2ik\pi/P)\rangle$ is a coherent state with displacement $-\Pi\alpha \exp(2ik\pi/P)$. Obviously, the multi-component MQS states can be obtained by adjusting the coupling ratio between self-interaction strength in the BEC and the impurities-BEC interaction strength. For a large amplitude of the initial coherent state of the BEC matter field mode, the quantum superposition states are macroscopically distinguishable.

Thus, the preparation of BEC P-component MQS states needs to meet two preconditions. Firstly, impurities need to be decoupled from BEC. This requires $t\kappa N = 2k\pi(k \in Z)$ according to Equations (13) and (14). We temporarily mark the moment of decoupling between impurities and BEC as t_d for convenience of description. Secondly, at the special decoupling moment t_d, the Kerr-interaction strength within the BEC needs to satisfy $t_d\lambda = \pi/P$ $(P = 2, 3, 4, \cdots, \infty)$.

Reviewing the preparation process of the above mentioned condensate *P*-component MQS states, we find that the impurities in BEC play a quantum catalytic [62] role in the context of interconversion of BEC quantum states. The catalytic effect of impurities is reflected in the following two aspects. On the one hand, the state of impurity at time t_d is the same as the initial state. That means the initial state $|\mathbf{GHZ}\rangle$ of impurities, just like a catalyst in a chemical process, does not change after dynamic evolution in certain parameter ranges. On the other hand, one can shorten the actual preparation time by increasing impurities-BEC interaction κ or impurity number N, and keeping the $\lambda = \pi/t_d P$. Thus, the impurity can accelerate the preparation of BEC *P*-component MQS states.

3.2. Creating a Pair of Approximately Orthogonal Cat States

In the field of continuous-variable (CV) quantum information processing [11,63,64], one can encode logical qubits by the harmonic oscillator states. A CV quantum code is then a subspace of the oscillator Hilbert space that is used to protect quantum information against errors. Thus, the generation of a pair of CV orthogonal basic vectors in harmonic oscillator space is of great significance. According to Equation (18), one can obtain a pair of approximately orthogonal cat states by changing the impurity number parity Π. We denote the quantum state of Equation (18) as $|\Psi(\tau = 2\pi)_{odd(even),\alpha}\rangle_{1/2P}$ when N is odd(even) number. The inner product between $|\Psi(\tau = 2\pi)_{odd,\alpha}\rangle_{1/2P}$ and $|\Psi(\tau = 2\pi)_{even,\alpha}\rangle_{1/2P}$ is

$$
\left| {}_{1/2P}\langle \Psi(\tau = 2\pi)_{even,\alpha} | \Psi(\tau = 2\pi)_{odd,\alpha}\rangle_{1/2P} \right|
$$
$$
= \frac{e^{-|\alpha|^2}}{P} \left| \sum_{k,s=1}^{P} e^{i[\xi_k - \xi_s - |\alpha|^2 \sin\theta]} e^{-|\alpha|^2 \cos\theta} \right|, \tag{19}
$$

where P, k, and s are positive integers. θ is defined as $2\pi(k-s)/P$. According to the right side of Equation (19), we can get a variety of inner product results for different values of P.

For example, if $P = 2$, Equation (19) takes the form

$$
e^{-i\pi n^2/2} = \frac{1}{2}(1-i) + \frac{1}{2}(1+i)(-1)^n. \tag{20}
$$

Then, $|\Psi(\tau = 2\pi)_{N,\alpha}\rangle_{1/4}$ can be rewritten as

$$
|\Psi(\tau = 2\pi)_{N,\alpha}\rangle_{1/4} = \frac{1-i}{2}|\Pi\alpha\rangle + \frac{1+i}{2}|-\Pi\alpha\rangle. \tag{21}
$$

Equation (21) is a superposition of two Glauber coherent states with the opposite direction in the phase space, i.e., the two-component MQS states of BEC. The inner product between $|\Psi(\tau = 2\pi)_{odd,\alpha}\rangle_{1/4}$ and $|\Psi(\tau = 2\pi)_{even,\alpha}\rangle_{1/4}$ is

$$
\left| {}_{1/4}\langle \Psi(\tau = 2\pi)_{even,\alpha} | \Psi(\tau = 2\pi)_{odd,\alpha}\rangle_{1/4} \right| = e^{-2|\alpha|^2}. \tag{22}
$$

For $\alpha = 4$, we have $e^{-2\alpha^2} = 1.266 \times 10^{-14}$ such that $|\Psi(\tau = 2\pi)_{odd,\alpha}\rangle_{1/4}$ and $|\Psi(\tau = 2\pi)_{even,\alpha}\rangle_{1/4}$ can be considered approximately orthogonal cat states. Thus, we can encode qubit logical states $|0\rangle = |\Psi(\tau = 2\pi)_{odd,\alpha}\rangle_{1/4}$ and $|1\rangle = |\Psi(\tau = 2\pi)_{even,\alpha}\rangle_{1/4}$ for $\alpha \geq 4$.

When $P = 4$, we have

$$
e^{-i\pi n^2/4} = \frac{1}{2}e^{-i(\pi/4)}[1-(-1)^n] + \frac{1}{2}(-i)^n[1+(-1)^n]. \tag{23}
$$

In this case, a four-component MQS state is obtained

$$
\begin{aligned}
|\Psi(\tau = 2\pi)_{N,\alpha}\rangle_{1/8} &= \frac{1}{2}e^{-i(\pi/4)}[|\Pi\alpha\rangle - |-\Pi\alpha\rangle] \\
&\quad + \frac{1}{2}[|-i\Pi\alpha\rangle + |i\Pi\alpha\rangle].
\end{aligned}
\tag{24}
$$

The inner product between $\left|\Psi(\tau = 2\pi)_{odd,\alpha}\right\rangle_{1/8}$ and $\left|\Psi(\tau = 2\pi)_{even,\alpha}\right\rangle_{1/8}$ is

$$
\left| {}_{1/8}\left\langle \Psi(\tau = 2\pi)_{even,\alpha} \middle| \Psi(\tau = 2\pi)_{odd,\alpha} \right\rangle_{1/8} \right| = e^{-2|\alpha|^2}.
\tag{25}
$$

Obviously, for large α, the MQS states of the same component corresponding to different impurities number parities are approximately orthogonal. Thus, one can generate a pair of approximately orthogonal CV cat states by changing the impurity number parity in our situation.

4. Engineering MQS States in Phase Space

4.1. Wigner Function of MQS States

The non-classicality of the MQS states also can be manipulated by the impurities number parity. We find that the Wigner function [65,66] distribution of $\left|\Psi(\tau = 2\pi)_{odd,\alpha}\right\rangle_{1/2P}$ is differs from $\left|\Psi(\tau = 2\pi)_{even,\alpha}\right\rangle_{1/2P}$ by π phase in phase space. Firstly, taking the two-component MQS state Equation (21) as an example, we analytically and graphically show the effect of impurities number parity on non-classicality by calculating Wigner function. The Wigner function has turned out to be remarkably useful in quantum physics, particularly in the characterization and visualization of nonclassical fields. The negativity of the Wigner function for a quantum state represents its non-classicality. The Wigner function is defined by

$$
W(z) = \frac{2}{\pi}\mathrm{Tr}\left[\hat{D}^\dagger(z)\rho\hat{D}(z)\hat{P}\right],
\tag{26}
$$

where ρ is the density operator of BEC in our situation, $\hat{D}(z) = \exp(z\hat{a}^\dagger - z^*\hat{a})$ and $\hat{P} = (-1)^{\hat{a}^\dagger\hat{a}}$ are the displacement operator and the parity operator, respectively.

The Wigner function of the two-component MQS state Equation (21) can be expressed as the sum of classical term and quantum interference term [67,68]

$$
W(z) = W_C(z) + W_Q(z).
\tag{27}
$$

For two-component MQS state Equation (21), the classical term is the sum of the independent Wigner functions of two Glauber coherent states $|\Pi\alpha\rangle$ and $|-\Pi\alpha\rangle$

$$
W_C(z) = \frac{1}{2}[W_1(z, \Pi\alpha) + W_2(z, -\Pi\alpha)].
\tag{28}
$$

$W_1(z, \Pi\alpha)$ and $W_2(z, -\Pi\alpha)$ are expressed as

$$
W_1(z, \Pi\alpha) = \frac{2}{\pi}\exp\left(-2\left|z - \Pi\alpha\right|^2\right),
\tag{29}
$$

$$
W_2(z, -\Pi\alpha) = \frac{2}{\pi}\exp\left(-2\left|z + \Pi\alpha\right|^2\right).
\tag{30}
$$

From Equations (29) and (30), we can see that the classical part of Equation (21)'s Wigner function consists of two Gaussian peaks, which centers are $z_1 = \Pi\alpha$ and $z_2 = -\Pi\alpha$, respectively. It can be found that the points z_1 and z_2 are symmetrical about the origin. As the impurity number parity parameter Π changes, the positions of the two Gaussian peaks will be transformed symmetrically about the origin.

The quantum interference term in the Wigner function of the MQS state Equation (21) consists of a cross term in the Wigner function, it can be expressed as

$$W_Q(z) = W_{21}(z; -\Pi\alpha, \Pi\alpha), \tag{31}$$

where $W_{21}(z; -\Pi\alpha, \Pi\alpha)$ is specifically expressed as

$$W_{21}(z; -\Pi\alpha, \Pi\alpha) = \frac{2}{\pi} \exp\left[-2\left(x^2 + y^2\right)\right] \tag{32}$$
$$\times \sin[4\Pi(x\alpha^y - y\alpha^x)].$$

We have defined $x = \mathbf{Re}(z), y = \mathbf{Im}(z)$ and $\alpha^x = \mathbf{Re}(\alpha), \alpha^y = \mathbf{Im}(\alpha)$. Quantum interference term Equation (31) depends on the phase superposition of two Glauber coherent states $\exp(-i\pi/4)|\Pi\alpha\rangle/\sqrt{2}$ and $\exp(i\pi/4)|-\Pi\alpha\rangle/\sqrt{2}$ in Equation (21). The Wigner function of Equation (21) is the sum of Equation (28) and (31), which is not positive definite, and the negativity comes from the quantum interference term. The change of the impurity number parity parameter Π causes the quantum interference mode in the phase space to produce a symmetrical transformation about the origin. Combined with the influence of Π on the classical part of the state Equation (21)'s Wigner function, it is found that the change of Π will induce the distribution of the quantum state Equation (21) in the phase space to produce a rotation of π angle.

In Figure 1, we have plotted the interference fringes of Equation (31) in a certain region of the phase space. One can find that the negative value and the positive value area in the phase space will be exchanged when the parity parameter Π changes.
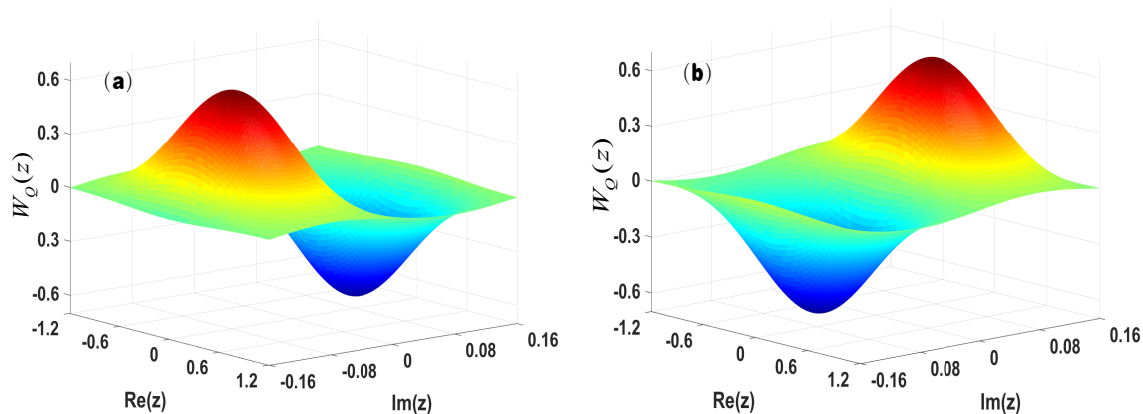

Figure 1. The quantum interference part of the Wigner function of quantum state Equation (21). The initial-state parameter of the BEC is $\alpha = 5$. The impurity number parity are chosen as (**a**) $\Pi = 1$ and (**b**) $\Pi = -1$.

For multi-component cases, the Wigner function of state Equation (18) can be expressed as

$$W_k(z; \Pi\alpha_k) = \frac{2}{\pi} \exp\left(-2\left|x - \Pi\alpha_k^x + i\left(y - \Pi\alpha_k^y\right)\right|^2\right), \tag{33}$$

$$W_{jk}(z; \Pi\alpha_j, \Pi\alpha_k) = \frac{2}{\pi} \exp\left(-2\left|x - \Pi\frac{\alpha_k^x + \alpha_j^x}{2} + i\left(y - \Pi\frac{\alpha_k^y + \alpha_j^y}{2}\right)\right|^2\right)$$
$$\times \cos\left[2\Pi\left(x\alpha_k^y - y\alpha_k^x\right) - 2\Pi\left(x\alpha_j^y - y\alpha_j^x\right) + \xi_k - \xi_j + \alpha_k^x\alpha_j^y - \alpha_k^y\alpha_j^x\right], \tag{34}$$

$$W(z; \Pi\alpha_1, \cdots, \Pi\alpha_P) = \frac{1}{P} \left[\sum_{k=1}^{P} W_k(z; \Pi\alpha_k) + 2 \sum_{\substack{j,k=1 \\ j>k}}^{P} W_{jk}(z; \Pi\alpha_j, \Pi\alpha_k) \right],$$ (35)

where $\alpha_{k(j)}^x = \mathbf{Re}\left[\alpha_{k(j)}\right]$ and $\alpha_{k(j)}^y = \mathbf{Im}\left[\alpha_{k(j)}\right]$. Through a series of tedious mathematical calculations, according with Equation (33)-(35), we first found that the transformation of Π will induces the distribution of the MQS states in the phase space to produce a rotation of π angle for any number of superposition components. Especially in the two-component case, one can discover the peaks or deeps displacement of the quantum interference fringes in the Wigner function takes place with an increasing number of impurities. The fundamental reason behind it is that the change in the parity of the impurity atom number causes the quantum interference fringes to rotate by the angle π around the origin of the phase space.

Secondly, according to Equation (34) and (35), we found that the number of interference terms in the Wigner function is related to the impurity-BEC coupling strength κ when the kerr nonlinearity strength λ inside the BEC is fixed. Specifically, P-component MQS state has $P(P-1)/2$ interference terms. Each interference term will form an obvious interference region within a certain phase space region. Thus, the value of P can be determined by the number of interference regions in the phase space. Then, the value of κ can be obtained by the ratio $\lambda/\kappa = 1/2P$, where λ can be treated as a constant. Hence, the quantum interference patterns are very sensitive to the number of impurity atoms and impurity-BEC coupling strength. In this sense, the quantum interference patterns in the phase space provide a possible way to probe the parity of the impurity atom number in the BEC and impurity-BEC coupling strength.

4.2. The Transition between Classic Mixed and Quantum Superposition

The transformation between classic and quantum is a fundamental problem of quantum theory. In this section, we will show that the switching of impurity number parity Π induces the transition of the BEC's state between classic mixed and quantum superposition. The state of BEC at time t can be obtained by tracing out the impurity part from the wave function $|\Psi(t)\rangle$, which is the wave function of impurities-doped BEC system at time t. Then the BEC state at time t is given by

$$\rho_B(\tau) = \frac{1}{2} e^{-|\alpha|^2} \sum_{n,m=0}^{\infty} e^{i\theta_{nm}\tau} \frac{\beta^n \beta^{*m} + \beta^{*n}\beta^m}{\sqrt{n!m!}} |n\rangle\langle m|,$$ (36)

where we have defined the scaled time $\tau = \kappa t$ and parameter θ_{nm} and β as following

$$\theta_{nm} = \frac{\lambda}{\kappa}\left(m^2 - n^2\right),$$ (37)

$$\beta = \alpha \exp(i\tau N/2).$$ (38)

Firstly, we assume that the scaled time $\tau = \pi$ and self-interaction strength $\lambda = 0.5\kappa$ in the BEC. Then, the density operator $\rho_B(\tau)$ can be rewritten as

$$\rho_B(\pi) = \frac{1}{2} e^{-|\alpha|^2} \sum_{n,m=0}^{\infty} e^{i\frac{\pi}{2}\left(m^2-n^2\right)} \frac{\left(\alpha e^{i\frac{\pi N}{2}}\right)^n \left(\alpha e^{-i\frac{\pi N}{2}}\right)^m + c.c.}{\sqrt{n!m!}} |n\rangle\langle m|.$$ (39)

If N is odd number, N can be rewritten as $N = 2k+1$ ($k \in \mathbf{N}$), $\rho_B(\pi)$ can be simplified as

$$\rho_B^{odd}(\pi) = \frac{1}{2}\left(|i\alpha\rangle\langle i\alpha| + |-i\alpha\rangle\langle -i\alpha|\right).$$ (40)

When N is even number, N can be rewritten as $N = 2k$ ($k \in \mathbf{N}$), $\rho_B(\pi)$ can be simplified as

$$\rho_B^{even}(\pi) = |\Psi_B^{even}(\pi)\rangle\langle\Psi_B^{even}(\pi)|, \tag{41}$$

and

$$|\Psi_B^{even}(\pi)\rangle = \frac{1}{2}\left[(1-i)\left|(-1)^k\alpha\right\rangle + (1+i)\left|(-1)^{k+1}\alpha\right\rangle\right], \tag{42}$$

where superscript $odd(even)$ of $\rho_B^{odd(even)}(\pi)$ expresses that the quantity of impurity atoms N is an odd(even) number. One can find that $\rho_B^{odd}(\pi)$ is a classical mixed state, while $\rho_B^{even}(\pi)$ is a pure two-component MQS state. The difference in preconditions between $\rho_B^{odd}(\pi)$ and $\rho_B^{even}(\pi)$ only is the difference of parity of impurities N. Thus, the parity switching of quantity N of impurities induces the transition between MQS states and classical mixed states in this case.

In order to show more clearly the influence of the parity of impurity number N on the BEC state C-Q(Classic-Quantum) transformation, we will calculate the degree of non-classicality for the states Equations (40) and (42). According to [69,70], the non-classicality for some states can be precisely quantified by the volume V of the negative part of the Wigner function. And V is defined by the following integral formula

$$V = \frac{1}{2}\int\int dq dp[|W(p,q)| - W(p,q)], \tag{43}$$

where q and p are position and momentum, respectively.

Here, in Figure 2, we plot the negative volume V as a function of the BEC initial coherent state parameter α for different parity of N by using numerical evaluation to complete it. "even" and "odd" in the legend indicate that the number of impurity atoms N is even number and odd number, respectively. Figure 2 clearly shows that the non-classical degree of Equation (40) disappears when N is an odd number. This quantity vanishes whenever the Wigner function is positive. However, when N takes an even number, the non-classical degree of Equation (42) gradually increases with the increase of α until limit value $V = 0.32$. In Figure 3, we plot the Wigner function of quantum state Equations (42) and (40). One can easily find that the Wigner function in Figure 3a has some negative parts, which corresponds to the non-classical nature of the state Equation (42). However, the Wigner function of Equation (40) in Figure 3b is positive semidefinite, which is attributed to the fact that state Equation (40) is a classical mixed state. The existence of non-classical degree is an intuitive manifestation of the characteristics of quantum superposition. To a certain extent, the parity of impurity number can determine the degree to which the BEC wave function deviates from the classic world.
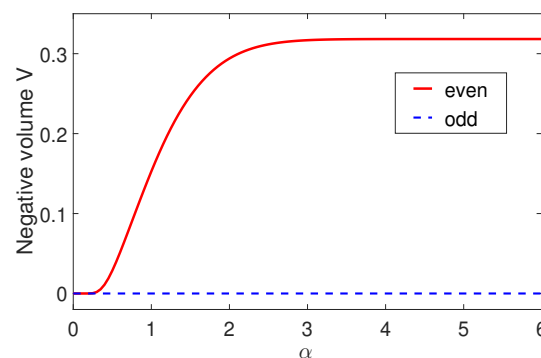

Figure 2. Negative volumes V of Wigner function of $\rho_B^{even}(\pi)$ and $\rho_B^{odd}(\pi)$ as a function of the parameter α. The number of impurity atoms N are even number and odd number corresponding to red solid and blue dashed line.
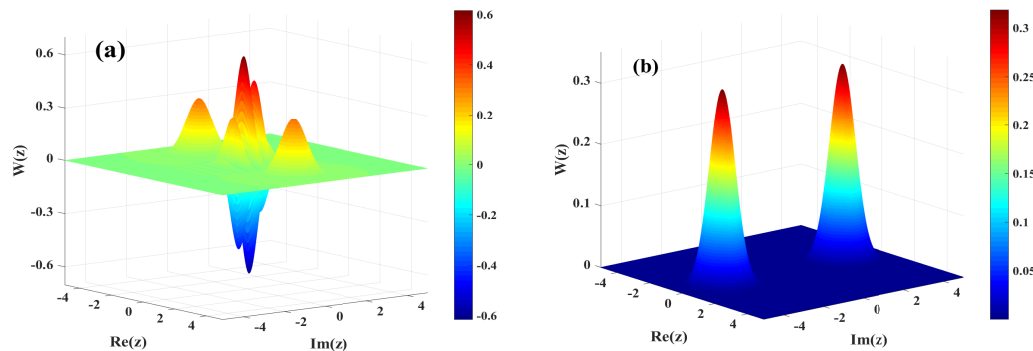
Figure 3. The Wigner function of quantum state Equations (42) and (40) plotted with different values of impurity atom number N. The initial-state parameter of the BEC is $\alpha = 3$. The number N of impurity atoms in figure (**a**,**b**) are even number and odd number, respectively.

5. Fast Generation of High-Fidelity MQS States in Open Systems

No quantum system is totally isolated. The interaction between the quantum system and the environment will occur in dynamic evolution. Then, this interaction will cause decoherence in the quantum system. In this section, we take into account the influence of the BEC decoherence on the generation of MQS states. In the present case, we assume the weak environment coupling and the Born-Markov approximation. The BEC is connected with a vacuum bath. The dominant decoherence source of the BEC is the atom loss due to inelastic collisions. When the BEC decoherence is considered, the dynamic evolution of the system is described by the master equation [48,71–73]

$$\dot{\rho} = -\frac{i}{\hbar}[H, \rho] + \mathcal{L}(\rho), \tag{44}$$

where the superoperator $\mathcal{L}(\rho)$ is given by

$$\mathcal{L}(\rho) = \gamma \left(a\rho a^\dagger - \frac{1}{2}a^\dagger a\rho - \frac{1}{2}\rho a^\dagger a \right), \tag{45}$$

and γ is the decay factor of the BEC, a is the BEC annihilation operator. The master equation and the reduced density operator $\rho_B(t) = \text{Tr}_{impurity}[\rho(t)]$ of the BEC matter field both can be calculated by Qutip [74,75].

In order to further confirm the degree of deviation of the generated state from the target state caused by BEC decoherence, the fidelity between the generated BEC state ρ_B and the target state $|\Psi(\tau = 2\pi)_{N,\alpha}\rangle$ is introduced by

$$F = \left\langle \Psi(\tau = 2\pi)_{N,\alpha} \middle| \rho_B \middle| \Psi(\tau = 2\pi)_{N,\alpha} \right\rangle. \tag{46}$$

Figure 4 shows that the fidelity between the generated state ρ_B and the target state $|\Psi(\tau = 2\pi)_{N,\alpha}\rangle$ will decreases with the increase of decay factor γ. So, the increase of the parameter γ is not conducive to the generation of the target MQS states. Given the negative effect of the environment on the generation of target MQS states, we will propose a scheme to reduce the influence of BEC decoherence so that the MQS states can be generated closer to the target states.

Taking the generation of the two-component MQS state as example, the preconditions of generating two-component MQS state Equation (21) are scaled time $\tau = \kappa t = 2\pi$ and ratio $\lambda/\kappa = 1/4$ in our case. One can find that the increase of impurities-BEC interaction κ and keeping the ratio $\lambda/\kappa = 1/4$ can shorten the actual time, which is required to generate Equation (21). The significantly shortened generation time allows us to achieve such states, which will be closer to the target state, within a typical coherence time of the system under BEC decoherence. After a certain numerical evaluation, Figure 5 shows that the increasing

of κ can effectively enhance the fidelity between target state Equation (21) and the generated BEC state $\rho_R(2\pi/\kappa)$ when BEC decoherence is considered.
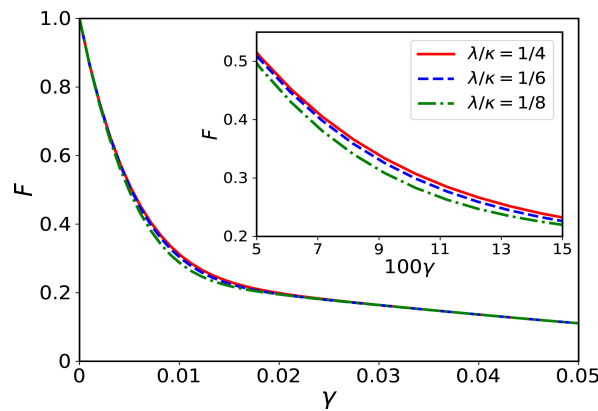

Figure 4. (Color online) The fidelity F as a function of γ at time $t = 2\pi/\kappa$. The other parameters are the same as Figure 1.
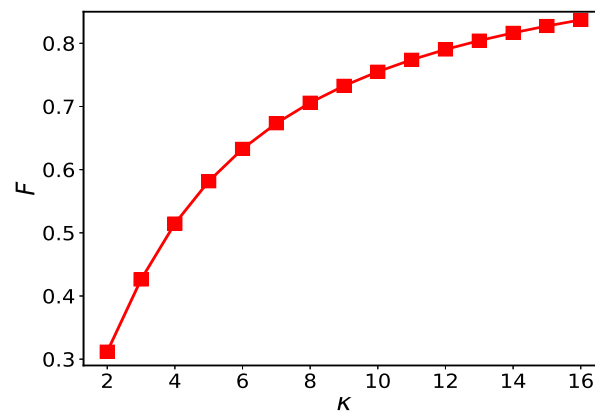

Figure 5. The fidelity F as a function of κ at time $t = 2\pi/\kappa$. The other parameters are $\alpha = 10$, $\lambda/\kappa = 1/4$, and $\gamma = 0.01$.

The enhancement of the impurity-BEC interaction can reduce the actual time, which is required to generate the MQS state. The physical mechanism behind it is that the period of entanglement between impurities and BEC is inversely proportional to κ when the quantity of impurity is fixed. Therefore, the increase of κ will lead to the advance of decoupling. Firstly, accelerating decoupling is conducive to the fast generation of MQS states. Secondly, the influence of the environment on the quantum system is a kind of accumulative effect in quantum system dynamic evolution processes. The fast generation [53] of MQS states can reduce the negative effect of the environment as far as possible. Thus, the quantum state ρ_B will be accomplished faster and approach the target state $|\Psi(\tau = 2\pi)_{N,\alpha}\rangle$ closer along with the enhancing of κ. It is worth noting that the results in Figure 5 are independent of the number N of impurity atoms. Because we have assumed in the previous discussion that the time point of the completely decoupling between the BEC and the impurity is $\tau = 2\pi$, which is independent of the number N of impurity atoms. Since Figure 5 is obtained by numerical calculation, we need to give a certain value of N to ensure the normal operation of the program. Here, we assume $N = 1$. However, the acceleration of system dynamics evolution can lead to the MQS live for a shorter time. Overcoming this flaw will also be one of the problems we need to solve in the future.

Figure 6 shows that the fidelity F is periodic in closed system. The points of $t = \pi/4$ and $t = 5\pi/4$ are the moment of decoupling between impurity and BEC, where the fidelity $F = 1$. This means that the distance between the target state and the generated state is zero

at time $t = \pi/4$ and $t = 5\pi/4$. As the decoherence parameter γ increaseing, the overall fidelity between the target and the generated states decreases in open system. Especially, the fidelity at time $t = 5\pi/4$ is much lower than $t = \pi/4$ due to the accumulation effect of the external environment. Thus, the fast generation of MQS states is beneficial to improve fidelity.
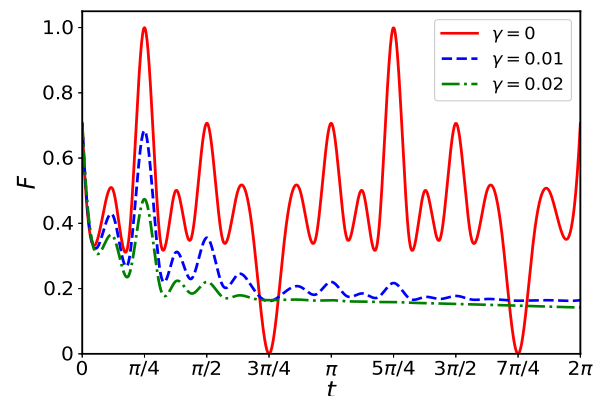

Figure 6. The fidelity F as a function of time t at $\kappa = 8$. The other parameters are $\alpha = 10$, $\lambda/\kappa = 1/4$, and $\gamma = 0$ (red solid line), 0.01 (blue dashed line), 0.02 (green dotdashed line).

6. Conclusions

We have studied the engineering of MQS states in an impurities-doped BEC system, which consists of BEC and N identical two-level immersed impurities. In our scheme, the interaction between impurities and BEC is a kind of coherent collision. When the initial states of impurities and BEC are GHZ state and coherent state, respectively, they are entangled periodically in the process of dynamic evolution. After a full period, the entanglement disappears, and the BEC is deterministically prepared in transient multi-component MQS states. The number of superposition components of the MQS states is determined by the ratio of the Kerr-type interaction within the BEC and the interaction between the impurities and BEC. Macroscopic quantum superposition in other kerr-type systems [76,77] is one of our future research directions. However, there are certain difficulties in preparing BEC to coherent state at present. We look forward to overcoming this difficulty in the future.

The immersion of impurities provides a new controllable degree of freedom for the manipulation of the MQS states. Firstly, a pair of approximately orthogonal CV cat states can be prepared by changing the impurity number parity. Secondly, we have analytically calculated the Wigner function of the BEC MQS states. The transformation of impurity number parity will induces the distribution of the MQS states in the phase space to produce a rotation of π angle for any number of superposition components. Thirdly, we have numerically calculated the degree of non-classicality by the negative volume of the Wigner function. The parity of the impurity number is the switch of the nonclassical degree of the BEC state. The switching of impurity number parity induces the transition of the BEC state between classic mixed and quantum superposition.

In the open system, the generation of MQS states is hindered. Due to the influence of the environment, the fidelity between the actually generated state and the target state will get worse. However, the interaction of impurities-BEC can reduce the influence of the environment so that the robustness of the system is enhanced. Specifically, not only is the fidelity improved, but also the preparation time is shortened with the increase of impurity-BEC interaction strength. Our results obtained in the present paper provides a versatile route to engineering MQS states of the BEC system through impurities.

Author Contributions: The contributions of author Z.L. are Conceptualization, methodology, validation and formal analysis. The contributions of author W.L. are software and data curation. All authors have read and agreed to the published version of the manuscript.

References

1. Dirac, P.A.M. *The Principles of Quantum Mechanics*; Oxford University Press: Oxford, UK, 1958.
2. Zurek, W.H. Decoherence and the Transition from Quantum to Classical. *Phys. Today* **1991**, *44*, 36.
3. Schrödinger, E. Die gegenwärtige Situation in der Quantenmechanik. *Naturwissenschaften* **1935**, *23*, 807.
4. Ghobadi, R.; Kumar, S.; Pepper, B.; Bouwmeester, D.; Lvovsky, A.I.; Simon, C. Optomechanical Micro-Macro Entanglement. *Phys. Rev. Lett.* **2014**, *112*, 080503.
5. Stobińska, M.; Jeong, H.; Ralph, T.C. Violation of Bell's inequality using classical measurements and nonlinear local operations. *Phys. Rev. A* **2007**, *75*, 052105.
6. Jeong, H.; Son, W.; Kim, M.S.; Ahn, D.; Brukner, Č. Quantum nonlocality test for continuous-variable states with dichotomic observables. *Phys. Rev. A* **2003**, *67*, 012106.
7. Vlastakis, B.; Kirchmair, G.; Leghtas, Z.; Nigg, S.E.; Frunzio, L.; Girvin, S.M.; Mirrahimi, M.; Devoret, M.H.; Schoelkopf, R.J. Deterministically Encoding Quantum Information Using 100-Photon Schrödinger Cat States. *Science* **2013**, *342*, 607.
8. Leghtas, Z.; Kirchmair, G.; Vlastakis, B.; Schoelkopf, R.J.; Devoret, M.H.; Mirrahimi, M. Hardware-Efficient Autonomous Quantum Memory Protection. *Phys. Rev. Lett.* **2013**, *111*, 120501.
9. Albert, V.V.; Shu, C.; Krastanov, S.; Shen, C.; Liu, R.-B.; Yang, Z.-B.; Schoelkopf, R.J.; Mirrahimi, M.; Devoret, M.H.; Jiang, L. Holonomic Quantum Control with Continuous Variable Systems. *Phys. Rev. Lett.* **2016**, *116*, 140502.
10. Cai, W.; Ma, Y.; Wang, W.; Zou, C.-L.; Sun, L. Bosonic quantum error correction codes in superconducting quantum circuits. *Fund. Res.* **2021**, *1*, 50–67.
11. Albert, V.V.; Mundhada, S.O.; Grimm, A.; Touzard, S.; Devoret, M.H.; Jiang, L. Pair-cat codes: autonomous error-correction with low-order nonlinearity. *Quantum Sci. Technol.* **2019**, *4*, 035007.
12. Pezzè, L.; Smerzi, A.; Oberthaler, M.K.; Schmied, R.; Treutlein, P. Quantum metrology with nonclassical states of atomic ensembles. *Rev. Mod. Phys.* **2018**, *90*, 035005.
13. Facon, A.; Dietsche, E.-K.; Grosso, D.; Haroche, S.; Raimond, J.-M.; Brune, M.; Gleyzes, S. A sensitive electrometer based on a Rydberg atom in a Schrödinger-cat state. *Nature* **2016**, *535*, 262.
14. McConnell, R.; Zhang, H.; Ćuk, S.; Hu, J.; Schleier-Smith, M.H.; Vuletić, V. Generating entangled spin states for quantum metrology by single-photon detection. *Phys. Rev. A* **2013**, *88*, 063802.
15. Duan, L.M.; Lukin, M.D.; Cirac, J.I.; Zoller, P. Long-distance quantum communication with atomic ensembles and linear optics. *Nature* **2001**, *414*, 413.
16. van Enk, S.J.; Hirota, O. Entangled coherent states: Teleportation and decoherence. *Phys. Rev. A* **2001**, *64*, 022313.
17. D. J. Wineland, *Nobel Lecture: Superposition, entanglement, and raising Schrödinger's cat*, Rev. Mod. Phys. 85, 1103 (2013).
18. Fröwis, F.; Sekatski, P.; Dür, W.; Gisin, N.; Sangouard, N. Macroscopic quantum states: Measures, fragility, and implementations. *Rev. Mod. Phys.* **2018**, *90*, 025004.
19. Xie, H.; Shang, X.; Liao, C.G.; Chen, Z.H.; Lin, X.M. Macroscopic superposition states of a mechanical oscillator in an optomechanical system with quadratic coupling. *Phys. Rev. A* **2019**, *100*, 033803.
20. Omran, A.; Levine, H.; Keesling, A.; Semeghini, G.; Wang, T.T.; Ebadi, S.; Bernien, H.; Zibrov, A.S.; Pichler, H.; Choi, S.; et al. Generation and manipulation of Schrödinger cat states in Rydberg atom arrays. *Science* **2019**, *365*, 570.
21. Chen, Y.H.; Qin, W.; Wang, X.; Miranowicz, A.; Nori, F. Shortcuts to Adiabaticity for the Quantum Rabi Model: Efficient Generation of Giant Entangled Cat States via Parametric Amplification. *Phys. Rev. Lett.* **2021**, *126*, 023602.
22. Qin, W.; Miranowicz, A.; Jing, H.; Nori, F. Generating long-lived macroscopically distinct superposition states in atomic ensembles. *Phys. Rev. Lett.* **2021**, *127*, 093602.
23. Parkins, A.S.; Walls, D.F. The physics of trapped dilute-gas BoseDEinstein condensates. *Phys. Rep.* **1998**, *303*, 1.
24. Dalfovo, F.; Giorgini, S.; Pitaevskii, L.P.; Stringari, S. Theory of Bose-Einstein condensation in trapped gases. *Rev. Mod. Phys.* **1999**, *71*, 463.
25. Leggett, A.J. Bose-Einstein condensation in the alkali gases: Some fundamental concepts. *Rev. Mod. Phys.* **2001**, *73*, 307.
26. Cirac, J.I.; Lewenstein, M.; Mølmer, K.; Zoller, P. Quantum superposition states of Bose-Einstein condensates. *Phys. Rev. A* **1998**, *57*, 1208.
27. Gordon, D.; Savage, C.M. Creating macroscopic quantum superpositions with Bose-Einstein condensates. *Phys. Rev. A* **1999**, *59*, 4623.
28. Dalvit, D.A.R.; Dziarmaga, J.; Zurek, W.H. Decoherence in Bose-Einstein condensates: Towards bigger and better Schrödinger cats. *Phys. Rev. A* **2000**, *62*, 013607.

29. Louis, P.J.Y.; Brydon, P.M.R.; Savage, C.M. Macroscopic quantum superposition states in Bose-Einstein condensates: Decoherence and many modes. *Phys. Rev. A* **2001**, *64*, 053613.

30. Huang, Y.P.; Moore, M.G. Creation, detection, and decoherence of macroscopic quantum superposition states in double-well Bose-Einstein condensates. *Phys. Rev. A* **2006**, *73*, 023606.

31. Dunningham, J.; Hallwood, D. Creation of macroscopic superpositions of flow states with Bose-Einstein condensates. *Phys. Rev. A* **2006**, *74*, 023601.

32. Piazza, F.; Pezzé, L.; Smerzi, A. Macroscopic superpositions of phase states with Bose-Einstein condensates. *Phys. Rev. A* **2008**, *78*, 051601.

33. Csire, G.; Apagyi, B. Macroscopic quantum superpositon states of two-component Bose-Einstein condensates. *Phys. Rev. A* **2012**, *85*, 033613.

34. Nolan, S.P.; Haine, S.A. Generating macroscopic superpositions with interacting Bose-Einstein condensates: Multimode speedups and speed limits. *Phys. Rev. A* **2018**, *98*, 063606.

35. Calsamiglia, J.; Mackie, M.; Suominen, K. Superposition of Macroscopic Numbers of Atoms and Molecules. *Phys. Rev. Lett.* **2001**, *87*, 160403.

36. Bar-Gill, N.; Rao, D.D.B.; Kurizki, G. Single-atom-aided probe of the decoherence of a Bose-Einstein condensate. *Phys. Rev. Lett.* **2011**, *107*, 010404.

37. Lau, H.W.; Dutton, Z.; Wang, T.; Simon, C. Proposal for the Creation and Optical Detection of Spin Cat States in Bose-Einstein Condensates. *Phys. Rev. Lett.* **2014**, *113*, 090401.

38. Pezzè, L.; Gessner, M.; Feldmann, P.; Klempt, C.; Santos, L.; Smerzi, A. Heralded Generation of Macroscopic Superposition States in a Spinor Bose-Einstein Condensate. *Phys. Rev. Lett.* **2019**, *123*, 260403.

39. Balewski, J.B.; Krupp, A.T.; Gaj, A.; Peter, D.; Buchler, H.P.; Low, R.; Hofferberth, S.; Pfau, T. Coupling a single electron to a Bose-Einstein condensate. *Nature* **2013**, *502*, 664.

40. Spethmann, N.; Kindermann, F.; John, S.; Weber, C.; Meschede, D.; Widera, A. Dynamics of Single Neutral Impurity Atoms Immersed in an Ultracold Gas. *Phys. Rev. Lett.* **2012**, *109*, 235301.

41. Will, S.; Best, T.; Braun, S.; Schneider, U.; Bloch, I. Coherent Interaction of a Single Fermion with a Small Bosonic Field. *Phys. Rev. Lett.* **2011**, *106*, 115305.

42. Zipkes, C.; Palzer, S.; Sias, C.; Köhl, M. A trapped single ion inside a Bose-Einstein condensate. *Nature* **2010**, *464*, 388.

43. Chikkatur, A.P.; Gölitz, A.; Stamper-Kurn, D.M.; Inouye, S.; Gupta, S.; Ketterle, W. Suppression and Enhancement of Impurity Scattering in a Bose-Einstein Condensate. *Phys. Rev. Lett.* **2000**, *85*, 483.

44. Yuan, J.B.; Lu, W.J.; Song, Y.J.; Kuang, L.M. Single-impurity-induced Dicke quantum phase transition in a cavity-Bose-Einstein condensate. *Sci. Rep.* **2017**, *7*, 7404.

45. Li, Z.; Kuang, L.M. Controlling quantum coherence of a two-component Bose-Einstein condensate via an impurity atom. *Quantum Inf. Process.* **2020**, *19*, 188.

46. Li, Z.; Han, Y.; Kuang, L.M. Complementarity between micro-micro and micro-macro entanglement in a Bose-Einstein condensate with two Rydberg impurities. *Commun. Theor. Phys.* **2020**, *72*, 025101.

47. Han, Y.; Li, Z.; Kuang, L.M. Quantum dynamics of an impurity-doped Bose-Einstein condensate system. *Commun. Theor. Phys.* **2020**, *72*, 095102.

48. Ng, H.T.; Bose, S. Single-atom-aided probe of the decoherence of a Bose-Einstein condensate. *Phys. Rev. A* **2008**, *78*, 023610.

49. Bruderer, M.; Jaksch, D. Probing BEC phase fluctuations with atomic quantum dots. *New J. Phys.* **2006**, *8*, 87.

50. Song, Y.J.; Kuang, L.M. Controlling decoherence speed limit of a single impurity atom in a Bose-Einstein-condensate reservoir. *Ann. Phys.* **2019**, *531*, 1800423.

51. Vogt, T.; Viteau, M.; Chotia, A.; Zhao, J.; Comparat, D.; Pillet, P. Electric-Field Induced Dipole Blockade with Rydberg Atoms. *Phys. Rev. Lett.* **2007**, *99*, 073002.

52. Büchler, H.P.; Micheli, A.; Zoller, P. Three-body interactions with cold polar molecules. *Nat. Phys.* **2007**, *3*, 726.

53. Yukawa, E.; Milburn, G.J.; Nemoto, K. Fast macroscopic-superposition-state generation by coherent driving. *Phys. Rev. A* **2018**, *97*, 013820.

54. Titulaer, U.M.; Glauber, R.J. Density Operators for Coherent Fields. *Phys. Rev.* **1966**, *145*, 1041.

55. Bialynicka-Birula, Z. Properties of the Generalized Coherent State. *Phys. Rev.* **1968**, *173*, 1207.

56. Stoler, D. Generalized Coherent States. *Phys. Rev. D* **1971**, *4*, 2309.

57. Kuang, L.M.; Zhou, L. Generation of atom-photon entangled states in atomic Bose-Einstein condensate via electromagnetically induced transparency. *Phys. Rev. A* **2003**, *68*, 043606.

58. Kuang, L.M.; Chen, Z.B.; Pan, J.W. Generation of entangled coherent states for distant Bose-Einstein condensates via electromagnetically induced transparency. *Phys. Rev. A* **2007**, *76*, 052324.

59. Yurke, B.; Stoler, D. Generating quantum mechanical superpositions of macroscopically distinguishable states via amplitude dispersion. *Phys. Rev. Lett.* **1986**, *57*, 13.

60. Liao, J.Q.; Tian, L. Macroscopic quantum superposition in cavity optomechanics. *Phys. Rev. Lett.* **2016**, *116*, 163602.

61. Lee, K.S.; Kim, M.S.; Bǔzek, V. Amplification of multicomponent superpositions of coherent states of light with quantum amplifiers. *J. Opt. Soc. Am. B* **1994**, *11*, 6.

62. Bu, K.; Singh, U.; Wu, J. Catalytic coherence transformations. *Phys. Rev. A* **2016**, *93*, 042326.

63. Braunstein, S.L.; van Loock, P. Quantum information with continuous variables. *Rev. Mod. Phys.* **2005**, *77*, 513.
64. Weedbrook, C.; Pirandola, S.; García-Patrón, R.; Cerf, N.J.; Ralph, T.C.; Shapiro, J.H.; Lloyd, S. Gaussian quantum information. *Rev. Mod. Phys.* **2012**, *84*, 62.
65. Louisell, W.H. *Quantum Statistical Properties of Radiation*; Wiley, New York, NY, USA, 1973.
66. Hillery, M.; O'Connell, R.F.; Scully, M.O.; Wigner, E.P. Distribution functions in physics: Fundamentals. *Phys. Rep.* **1984**, *106*, 121.
67. Buzěk, V.; Knight, P.L. The origin of squeezing in a superposition of coherent states. *Opt. Commun.* **1991**, *81*, 5.
68. Buzěk, V.; Vidiella-Barranco, A.; Knight, P.L. Superpositions of coherent states: Squeezing and dissipation. *Phys. Rev. A* **1992**, *45*, 9.
69. Kenfack, A.; Życzkowski, K. Negativity of the Wigner function as an indicator of non-classicality. *J. Opt. B Quantum Semiclass. Opt.* **2004**, *6*, 396.
70. Meng, X.G.; Li, K.C.; Wang, J.S.; Zhang, X.Y.; Zhang, Z.T.; Yang, Z.S.; Liang, B.L. Continuous-Variable Entanglement and Wigner-Function Negativity via Adding or Subtracting Photons. *Ann. Phys.* **2020**, *532*, 1900585. https://doi.org/10.1002/andp.201900585.
71. Jack, M.W. Effect of atom loss on collapse and revivals of phase coherence in small atomic samples. *Phys. Rev. A* **2003**, *67*, 043612.
72. Jack, M.W. Decoherence due toThree-Body Loss and its Effect on the State of a Bose-Einstein Condensate. *Phys. Rev. Lett.* **2002**, *89*, 140402.
73. Wang, W.; Fu, L.B.; Yi, X.X. Effect of decoherence on the dynamics of Bose-Einstein condensates in a double-well potential. *Phys. Rev. A* **2007**, *75*, 045601.
74. Johansson, J.R.; Nation, P.D.; Nori, F. QuTiP: An open-source Python framework for the dynamics of open quantum systems. *Comput. Phys. Commun.* **2012**, *183*, 1760.
75. Johansson, J.R.; Nation, P.D.; Nori, F. QuTiP 2: A Python framework for the dynamics of open quantum systems. *Comput. Phys. Commun.* **2013**, *184*, 1234.
76. Gao, Y.P.; Liu, X.F.; Wang, T.J.; Cao, C.; Wang, C. Photon excitation and photon-blockade effects in optomagnonic microcavities. *Phys. Rev. A* **2019**, *100*, 043831.
77. Aldana, S.; Bruder, C.; Nunnenkamp, A. Equivalence between an optomechanical system and a Kerr medium. *Phys. Rev. A* **2013**, *88*, 043826.